Multiplexing with Multispectral Imaging: From Mice to Microscopy

Richard M. Levenson, David T. Lynch, Hisataka Kobayashi, Joseph M. Backer, Marina V. Backer

Abstract

Increasing sophistication in the design and application of biological models as well as the advent of novel fluorescent probes have led to new demands on molecular imaging systems to deliver enhanced sensitivity, reliable quantitation, and the ability to resolve multiple simultaneous signals. Sensitivity is limited, especially in the visible spectral range, by the presence of ubiquitous autofluorescence signals (mostly arising from the skin and gut), which need to be separated from those of targeted fluorophores. Fluorescence-based imaging is also affected by absorbing and scattering properties of tissue in both the visible and to a lesser extent the near-infrared (NIR) regions. However, the small size of typical animal models (usually mice) often permits the detection of enough light arising even from relatively deep locations to allow the capture of signals with an acceptable signal-to-noise ratio. Multispectral imaging, through its ability to separate autofluorescence from label fluorescence, can increase sensitivity as much as 300 times compared to conventional approaches, and concomitantly improve quantitative accuracy. In the NIR region, autofluorescence, while still significant, poses less of a problem. However, the task of disentangling signals from multiple fluorophores remains. Multispectral imaging allows the separation of five or more fluorophores, with each signal quantitated and visualized separately. Preclinical small animal imaging is often accompanied by microscopic analysis, both before and after the in vivo phase. This can involve tissue culture manipulations and/or histological examination of fixed or frozen tissue. Due to the same advantages in sensitivity, quantitation, and multiplexing, microscopy-based multispectral techniques form an excellent complement to in vivo imaging.

Key Words: autofluorescence; fluorescence; in vivo imaging; multiplexing; reagents

Richard M. Levenson, MD, is Director of Research and David T. Lynch, PhD, is Senior Scientist at CRI Inc. in Woburn, Massachusetts. Hisataka Kobayashi, MD, PhD, is a staff scientist in molecular imaging at the National Institutes of Health in Bethesda, Maryland. Joseph M. Backer, PhD, is Chief Executive Officer and Marina V. Backer, PhD, is Senior Scientist with SibTech Inc. in Newington, Connecticut.

Address correspondence and reprint requests to Dr. Richard M. Levenson, Director of Research, CRI Inc., 35B Cabot Road, Woburn, MA 01801 or email rlevenson@cri-inc.com.

Overview

Fundamental research into biological processes at the cellular level has transformed our understanding of disease pathology. However, while many of the biochemical pathways involved in disease processes are being elucidated in isolated cellular systems, it may be more appropriate to study the complexities of biomolecular signaling pathways and their pathogenic contribution at the tissue, organ, and system levels in intact vertebrate systems. Accordingly, with the advent of molecular and functional in vivo imaging, the scientific community is extending cell-based assays to small animal models in order to provide system-level contexts.

While there is certainly a basic science aspect to this work, clinical drug development increasingly relies on small animal imaging for many facets of lead qualification, efficacy assessments, toxicity determinations, and biomarker discovery and validation. Small mammals, typically mice and rats, thus play an important role in biomedical research. These models are desirable due to their low cost of maintenance and housing, short reproductive cycle, availability, and portability. Over the last decade, there has been a dramatic increase in mouse utilization, in part because of the flexibility of the mouse genome. The mouse genotype can be manipulated almost at will, providing a unique tool in evaluating the effects of targeted manipulations on the phenotype of a mammalian system. The widespread use of transgenic murine systems, along with the development of molecular reagents that can visualize and track probes in vivo, has spurred the development of numerous preclinical imaging systems.

The ability to perform relevant minimally or noninvasive imaging helps reduce costs and enables longitudinal studies of multiple processes and parameters in individual animals. Excellent reviews of the pros and cons of each of these methods are available (Balaban and Hampshire 2001; Weissleder and Mahmood 2001).

Animal imaging systems, whose technologies can involve ultrasound, nuclear imaging (both positron and single-photon tomography), x-ray computed tomography, magnetic resonance imaging techniques, and a variety of optical approaches, can be roughly categorized as having anatomical, functional, and/or molecular capabilities.

The anatomical methods that have become the diagnostic cornerstones of clinical medicine include x-ray, com-

puted tomography (CT[1]), magnetic resonance imaging (MRI), and ultrasound, all scaled for specialty use in small animal imaging. For the most part, however, these approaches, while useful for revealing anatomical features, are less relevant for elucidating molecular and cellular events, although this is changing rapidly due to the development of innovative chemistries and labeling strategies (Lecchi et al. 2007; Torigian et al. 2007).

The functional imaging technologies, which include optical techniques, can examine more dynamic processes such as perfusion, oxygenation, metabolism, and other more or less generic physiological processes. These can be extremely useful, as evidenced by the success of fluorodeoxyglucose (FDG) positron emission tomography (PET[1]), which can monitor tumor response to chemotherapy, for example, sometimes within hours after the first dose (Miller et al. 2007; Nanni et al. 2007; van der Weerdt et al. 2007; Wolz et al. 2007). The generic nature of these commonly used modalities facilitates their application in many different situations, but by the same token they do not convey information about more specific pathways or targets.

In vivo molecular imaging involves detecting specific molecular targets. Numerous modalities are capable of this, including MRI, PET and single photon emission computed tomography (SPECT), ultrasound (using tagged microbubbles; Klibanov 2005, Postema et al. 2005), and various optical approaches.

Recently, instrument manufacturers have striven to develop hybrid technologies that incorporate the use of two or more single-modality systems concurrently, such as fluorescence, bioluminescence, and/or PET-CT and SPECT-CT, to meet the demand of those attempting to extract the most information possible about a particular biochemical process (Del Guerra et al. 2000; Deroose et al. 2007). Each of these methods has strengths and weaknesses in terms of both functional utility and practicality. For example, while striking advances in MR and CT-based systems have occurred in recent years, there is still a significant cost burden associated with these approaches. Similarly, nuclear technologies such as PET or SPECT require significant investment in radiochemical capabilities and have relatively poor spatial resolution.

Optical methods, and particularly fluorescence-based methods, have a particular set of characteristics that, taken broadly, establish optical as one of the most versatile and effective imaging modalities for preclinical animal studies. This is the case for a variety of reasons, including cost and regulatory constraints, and is evidenced by the increasing use of optical imaging methods in small animal–based research and development.

In this article, we highlight the application of multispectral fluorescence-based imaging as a noninvasive small animal phenotyping tool, with an emphasis on multiplexed analysis and novel image processing tools for preclinical studies in mice. We focus on the mouse because it is the dominant mammalian model for human disease and its physical scale provides both challenges and opportunities in imaging sciences. One advantage that we will discuss is the capacity to visualize molecular labels on spatial scales that extend from the subcellular level to the whole animal.

Optical Techniques

Bioluminescence and Fluorescence

Optical molecular imaging systems and methods use both bioluminescent (Rice et al. 2001) and fluorescent (Graves et al. 2003) signals. Bioluminescent systems typically use luciferase genes coupled with luciferin substrates as reporters. The major attraction of this approach is that although absolute light levels generated by the targets may be low, photons are generated for the most part only where luciferase is present, leading to low background signals. In contrast, fluorescence-based imaging requires an external light source to stimulate the emission of light from the probe.

In addition to bioluminescence and fluorescence, another technique known as photoacoustic imaging (Zhang et al. 2006, 2007) is also under development. Based on intrinsic or extrinsic contrast mechanisms, it uses light to cause absorbers to heat up and expand rapidly, thereby generating a sound wave detected by surface acoustic transducers. Photoacoustic imaging is a promising approach but is still in its early days; therefore we do not discuss it further here.

Benefits and Challenges of Fluorescence-based Imaging

Benefit: Flexibility. Compared to bioluminescence, fluorescence is the more flexible technology, because it permits the use of a far wider range of probes, labeling methods, and targets, and can be used with labels that emit in the near-infrared (NIR[1]), the spectral "sweet spot" for deep tissue in vivo imaging (Ntziachristos et al. 2001, 2003).

Fluorescence-based methods are useful for imaging practically any of the fluorophores used in biomedical research, with best results typically achieved in vivo when the emission wavelengths of the dye are between 500 and 950 nm (Mansfield et al. 2005b), as blue and ultraviolet (UV) light signals penetrate tissue extremely poorly. It is possible to genetically encode these fluorophores in xenografts or express them in transgenic animals; attach them covalently to antibodies, peptides, or other agents that bind to targets; or introduce them exogenously as fluorescent dyes for targeting by various means. Gao and colleagues (2004) describe an example of antibody-targeted spectral imaging and analysis, examining the distribution of quantum dot–labeled antitumor antibodies in mice.

[1]Abbreviations used in this article: CCD, charge-coupled device; CT, computed tomography; LCTF, liquid crystal tunable filter; NIR, near-infrared; PET, positron emission tomography; QD, quantum dot; RGB, red-green-blue

Benefit: Multiplexing. Because biological processes are complex, it is often desirable, except in simple cases, to monitor more than one event or target at a time. For example, tumor location *and* expression of appropriate targetable surface markers *and* oxy-deoxy hemoglobin status *and* presence of necrosis or apoptosis *and* documentation of drug delivery might all be desired attributes to follow using in vivo imaging. Although capturing such a suite of simultaneous readouts is not yet feasible, multiplex capabilities such as these are not inconceivable and, in some implementations, could be achieved using injection of a cocktail of fluorescently labeled antibodies or other targeting agents. These would be separable using either their fluorescence spectra or lifetimes and could be independently visualized and quantitated. Quantum dots, a family of nanoparticles with size-tunable emissions extending into the NIR (Gao et al. 2002; Gao and Nie 2005), have promise in this area, although issues of toxicity and biodistribution require further research.

Benefit: Cost and speed. The intrinsic cost of fluorescent imaging systems can be low, at least compared to other modalities such as CT, MR, and PET/SPECT, because their most simple implementation is an inexpensive camera in a light-tight box. Speed is also an advantage, at least in some approaches, because signals can be relatively bright, and it is possible to image many mice (up to five or six) simultaneously and within seconds.

Benefit: Extended spatial scale. As noted above, fluorescent signals are suitable for examination at the whole-animal level, either by using in vivo microscopy or by examining tissues obtained by biopsy or necropsy. In some instances, if the in vivo label is reasonably photostable, positionally stable despite freezing or fixation and sectioning, and present in sufficient quantity to be visualized in thin sections, it is possible to detect the same labels both in vivo and in vitro, providing validation for both techniques.

Challenge: Imaging at depth. Many studies are best accomplished using planar (single-view) imaging, and the

Figure 1 Maestro™ in vivo imaging system. An LCTF-based multispectral camera system and excitation source can capture reflectance and fluorescence images of small animals at multiple wavelengths. Spectral analysis software can then "unmix" multiple signals, removing autofluorescence contributions and increasing sensitivity and quantitative accuracy.

choice of platform depends on the question being asked. Because photons are scattered and absorbed by biological tissues, most prominently in the visible range but also in the NIR, optical imaging is easiest to accomplish when signals arise from superficial sources—for example, subcutaneous tumor deposits or inflammatory processes in extremities. Deeper structures may be detectable (depending on the wavelengths used), but the signals can become very diffuse and hard to localize. Researchers are developing tomographic approaches for detecting, resolving, and quantitating signals at depth (Ntziachristos et al. 2002, 2005), but these are still a work in progress, and in comparison to planar imaging require longer exposure times and computationally intense image reconstruction. Although such approaches are promising, we do not address them in further detail here.

Challenge: Autofluorescence. The number of photons emitted with fluorescence is orders of magnitude greater than with bioluminescence; however, it is the presence of relatively bright autofluorescence that generally limits achievable target-to-background ratios (Troy et al. 2004). The ubiquitous autofluorescence signals that degrade performance in conventional fluorescence-based small animal imaging systems are mainly attributable to components of the skin (mostly collagen, which fluoresces primarily in the green) and to food (mostly chlorophyll-breakdown products) and porphyrins, both of which fluoresce primarily in the red. Thus, relatively dim green and red fluorescent molecular signals can be impossible to detect in intact small animals with conventional imaging approaches. The contribution from chlorophyll-related compounds can be reduced by switching the test subjects to one of a variety of specially formulated diets (Troy et al. 2004). While this is certainly helpful, a more general solution is to separate autofluorescence signals from those of greater interest by using time-resolved or multispectral techniques.

Multispectral Imaging

Multispectral imaging (MSI) is an approach that optimizes the opportunities for multiplexing while at the same time overcoming the effects of autofluorescence on detectability and reliable quantitation. While it is possible to acquire multispectral datasets by simply rotating a filter wheel in front of a charge-coupled device (CCD[1]) camera, the use of electronically tunable filters (no moving parts, continuous tunability) is attractive. After a multispectral image set is captured, spectral unmixing and signal quantitation and display complete the imaging process. We provide examples that illustrate how sensitivity in the face of autofluorescence is amplified, how multiple signals can be separated, and how microscopy can play a role in validation.

LCTF-based Spectral Imaging Hardware

Small animal imaging. The Maestro™ system (CRI, Woburn, MA) of multispectral approaches to small animal imaging (Figure 1) is based on the use of liquid crystal tunable filters (LCTFs[1]; for descriptions of LCTF core technology, see Miller and Hoyt 1995, Gat 2000, and Hoyt et al. 2001; Berman and Moore 1994 compare the LCTF method in some detail to other spectral imaging techniques).

Several features of LCTFs make them suitable choices for many situations. They are band-sequential filters that are easily coupled to focal plane array detectors that employ inexpensive and/or fast complementary metal-oxide-semiconductor (CMOS), standard CCD, or high-sensitivity, high-speed electron-multiplying CCD (EMCCD) technologies, among others. By sequentially tuning the filter and exposing the sensor, it is possible to acquire complete images at each wavelength, band by band. Unlike some other techniques (for example, those that use prisms or gratings to disperse and collect all wavelengths simultaneously), this design allows the user to vary the exposure time as a function of wavelength, thus optimizing the signal-to-noise ratio (SNR) in situations where sensitivity (emitted photons convolved by imaging receiver characteristics) varies over the spectral range. Moreover, the wavelengths acquired can be arbitrarily spaced through the spectral range of interest, allowing the user to maximize SNR by acquiring only the most informative bands (Miller and Harvey 2001). Other advantages include the absence of moving parts, excellent optical properties that yield near-diffraction-limited images (of particular importance for microscopy-based applications), spectral stability to fractions of a nanometer, and high reliability.

Figure 2 Nuance™ multispectral imaging system for microscopy. A spectral imaging camera similar to that inside the Maestro imager that mounts on any C-mount-equipped microscope (e.g., upright, inverted, or dissecting) provides multispectral imaging at the cellular and subcellular scale. The background and inset images illustrate a "before-and-after" example of the application of spectral unmixing to a fluorescence in situ hybridization (FISH) analysis of a breast cancer biopsy, separating tissue autofluorescence from fluorescently labeled nuclei, and Her2 and chromosome-17 molecular signals.

The remainder of the system consists of a cooled megapixel CCD camera, a Xenon-based excitation light source with interference-filter-selectable spectral ranges, heated stage and anesthesia manifold, and a light-tight enclosure. Because the tunable filter by itself displays the 6 logs of blocking required to exclude excitation light from the sensor, a long-pass emission filter (chosen to match the selected excitation filter) is also inserted in the light path in front of the tunable filter, which then spectrally resolves the transmitted emission light. As many as three mice can be imaged simultaneously. Alternatively, the field of view can be zoomed to about the size of a large postage stamp, so that a resolution of approximately 40 microns at the object is achievable if the unbinned 1,300 × 1,000–pixel resolution of the camera is employed.

Multispectral microscopy. The Nuance™ microscope-based imaging system (Figure 2) is similar in concept to the Maestro, except that the LCTF, optics, and a cooled megapixel CCD camera are integrated into a device that mounts on any microscope equipped with a C-mount adapter (commonly used for digital cameras). The spectral ranges for either the Maestro or Nuance systems can be selected to span either 420 to 720 nm (the visible range) or 500 to 950 nm (well suited for in vivo imaging). The Nuance system can also be used for brightfield (nonfluorescence) microscopy, with particular application to multiplexing chromogen-based immunohistochemistry studies (Taylor and Levenson 2006).

Most acquisitions involve automatically taking a series of exposures spaced 10 or 20 nm apart over the desired spectral range, and then saving the resulting spectral data "cube" in a proprietary format or, alternatively, as a series of TIFFs or a raw floating point file. Typical exposure times for small animal imaging range from ~5 to ~50 seconds for an entire multispectral dataset (up to 10 wavelengths, from 50 ms to 5 s per wavelength). If multiple fluorescent species are being imaged that require changing excitation wavelengths, the imaging will of course take somewhat longer. Microscope-based imaging usually entails somewhat shorter exposure times.

Tunable filters and throughput. There are some disadvantages related to band-sequential approaches in general and/or LCTFs in particular. A band-sequential approach implies that the complete image stack (or "cube") is built up

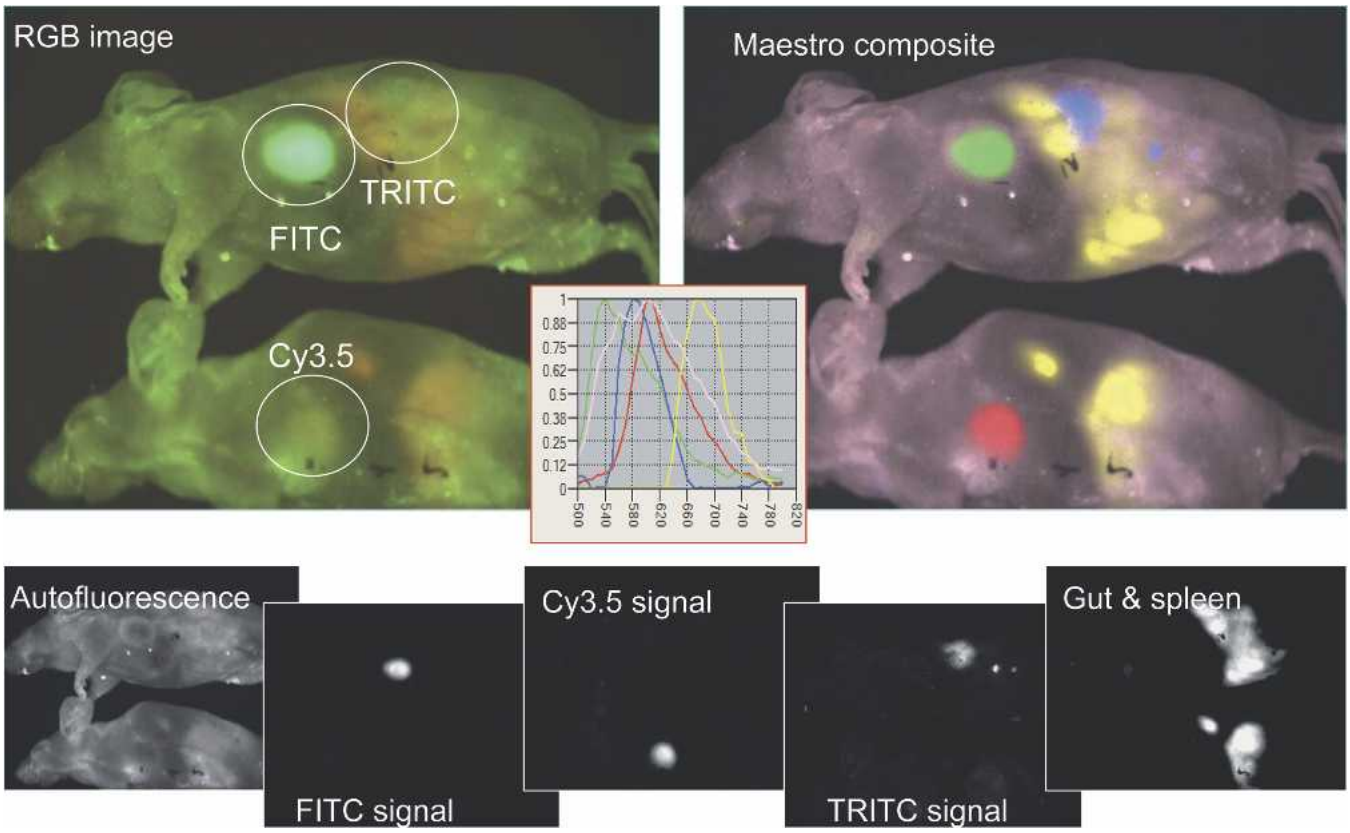

Figure 3 Nude mice with two different species of autofluorescence and three subcutaneous fluorophore signals. Two mice were injected subcutaneously with three fluorophores (FITC, TRITC, and Cy3.5) and spectrally imaged in a Maestro. The color image (top, left) indicates the appearance of the mice before spectral unmixing was performed. The inset (top, center) shows the spectra of all five major signals: skin autofluorescence (pink), and the "purified" spectra of FITC (green), TRITC (blue), Cy3.5 (red), and food (yellow) generated using the "Compute Pure Spectrum" (CPS) algorithm. Spectrally unmixed component images are shown in the bottom panels, and a pseudo-colored composite image is shown in the top row (right).

over time; thus, if significant sample or camera movement occurs during the acquisition, or if high temporal resolution is needed to capture certain events (e.g., calcium signaling transients), single-exposure ("snapshot") acquisition strategies could be more appropriate. Overall light throughput can be a concern: LCTFs use polarization in their spectral selection process, and transmission efficiencies are typically about 30%, in comparison to traditional interference filters that can transmit approximately 90% of incoming light.

However, the metric of success in imaging is usually not total photons captured but achievable SNR (or signal-to-background) within a given time, and except where high speed is required, the benefit of spectral information gained generally outweighs the impact of lower transmission efficiencies. For example, compare a grayscale to a color image: as much as two-thirds or so of the available light is lost in a color sensor due to the presence of red-green-blue filter masks over individual pixels. However, the useful information content of a color image, captured ultimately with fewer photons reaching the detector, can be vastly more than that of a monochrome image of the same scene.

Tuning time of the filter is approximately 50 ms, which is shorter than the typical exposure time for individual image planes (often 100 to 2,000 ms, depending on the brightness of the signal); total imaging times for typical imaging sessions range from 5 to 30 seconds. Other approaches to spectral imaging can include highly populated filter wheels, which have the benefit of improved throughput and high out-of-band rejection, and the disadvantage of requiring moving parts and lack of complete spectral flexibility. It is also possible to achieve spectral discrimination on the excitation side, which can be advantageous in that high-efficiency long-pass filters can be used on the emission side.

It is fair to say that all of these alternatives are effective, and that, especially in fluorescence, the problem is not the amount of light collected but how the signals are processed after collection.

Multispectral Analysis

Spectral cube display. A spectral data cube is a multidimensional dataset consisting of spatial information denoted by x,y coordinates, or pixels, and individual measured spectra at each of these pixels. There may be a lot of information in one of these datasets, which are amenable to analysis using a variety of straightforward or sophisticated methods. However, the two essential functions of spectral imaging software are to display the raw data in a visually interpretable image, and to unmix various signals into their own separate channels or component images. Because human vision is not able to interpret more than three color channels, it is necessary to display the high-dimensional spectral dataset in a red-green-blue (RGB[1]) color image. Either true-color (in which spectral regions are mapped faithfully into their corresponding RGB channels) or false-color displays can be generated; the latter are useful when signals in the near-infrared (by definition mostly invisible to human vision) are acquired. All the RGB images in this article are derived from spectral datasets and not from conventional color sensors.

Spectral unmixing. Spectral unmixing can faithfully separate signals that may overlap both spatially and spectrally, without "crosstalk" (i.e., signals from one label showing up in a channel ostensibly dedicated to another). The basic mathematical approach is part of the conventional (nonimaging) spectroscopic toolbox, and is at heart a simple least-squares fit that takes the measured (experimental) spectrum at each pixel and breaks it up as a linear combi-

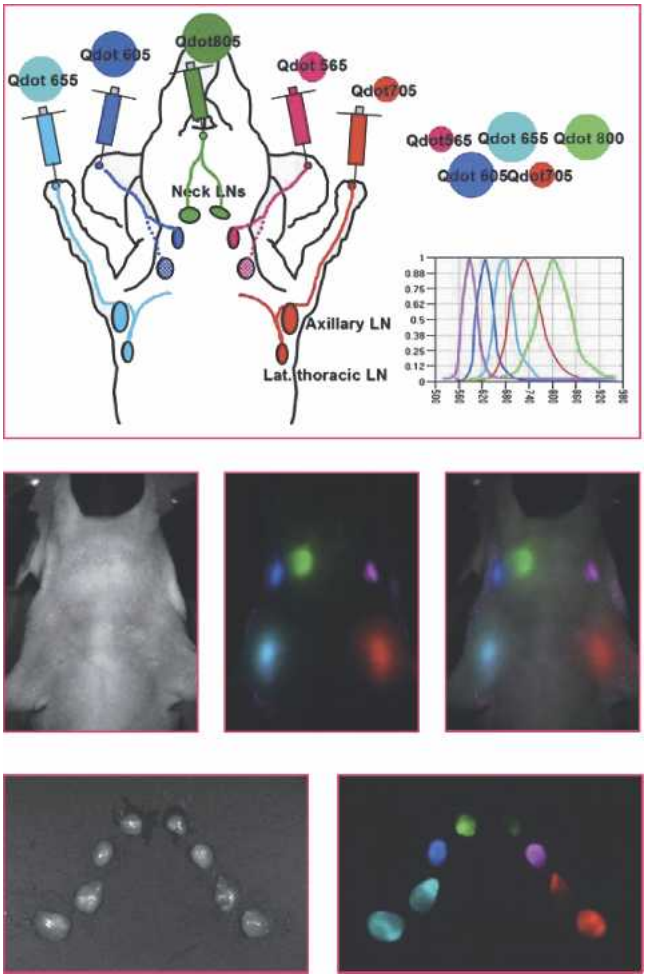

Figure 4 Five-color spectrally unmixed quantum dot detection of lymphatic system anatomy. Top: A schematic illustration of 5-color quantum dot lymphatic injection sites and draining destinations of spectral fluorescence imaging, with a graph of the emission spectra of each of the quantum dots used. Middle row: Five primary draining lymph nodes were simultaneously visualized with different colors as shown: autofluorescence image of mouse (left); composite pseudo-colored detection of draining lymph nodes after spectral unmixing (middle); image merge of the left and center panels (right). Bottom row: Reflectance (left) and spectrally unmixed and pseudo-colored image (right) of surgically dissected lymph nodes arranged in the same geometry as in the intact mouse.

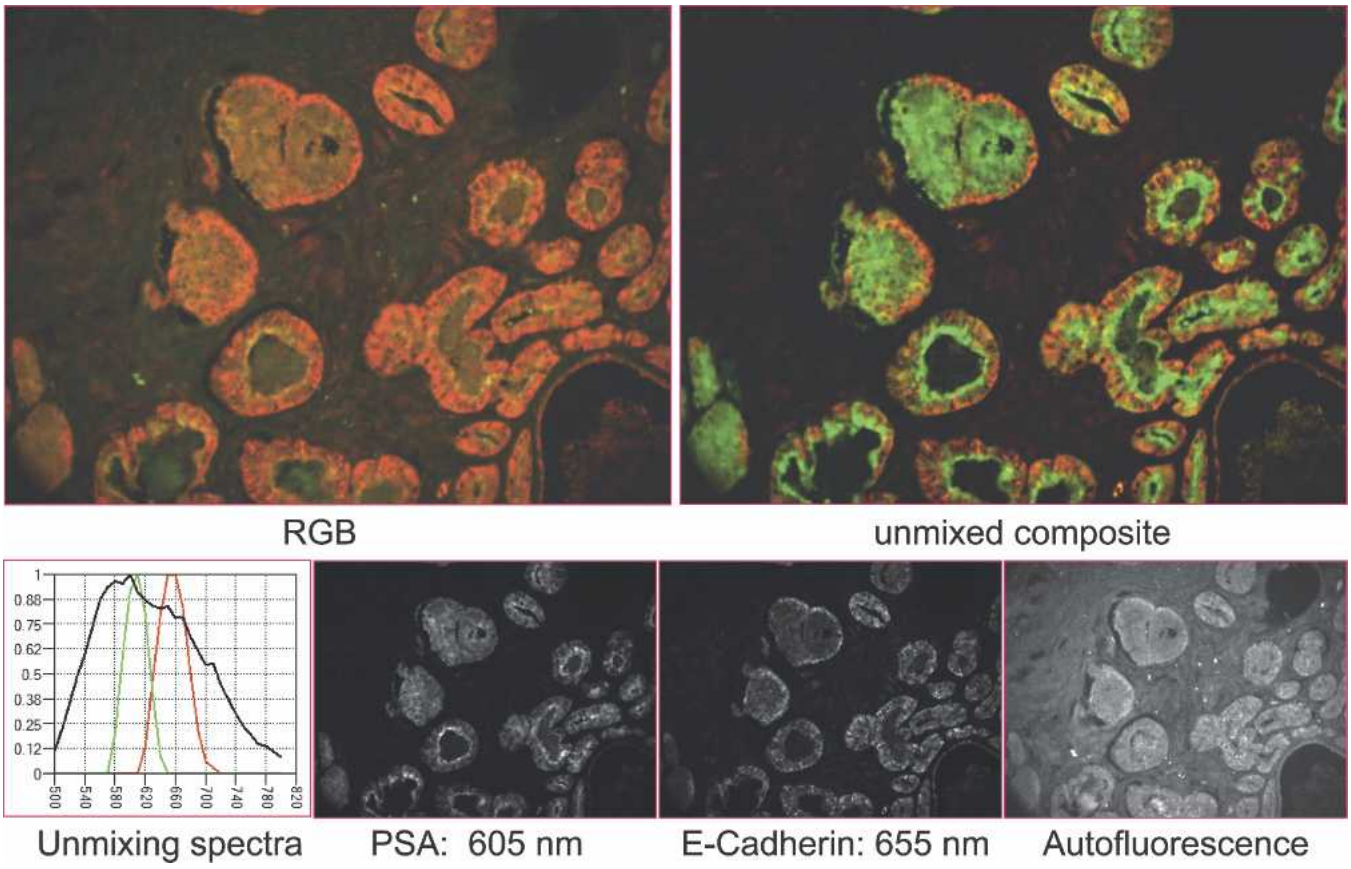

Figure 5 Spectral unmixing in microscopy. Prostate-specific antigen (PSA) and E-cadherin staining, visualized with quantum dot–labeled indirect immunofluorescence, in a section of formalin-fixed, paraffin-embedded human prostate cancer tissue. Top left: Color image of the sample before spectral unmixing. Bottom row: Spectra of 605-nm (green line) and 655-nm (red line) quantum dot labels as measured in this specimen, along with the autofluorescence spectrum of the tissue (black line); and three individual component images. A pseudo-colored composite image that combines the two quantum dot channels (but not the autofluorescence channel) is shown top right. RGB, red-green-blue.

nation of spectra corresponding to the signals expected to be present (Farkas et al. 1998). We add additional constraints (such as nonnegativity) to the unmixing algorithms, and also manage the residuals that represent how well a linear sum of spectral library members can recreate the actual (measured) spectra.

To ensure faithful unmixing results, it is essential to obtain accurate spectra representing each signal in the image. These can be provided to the software via established spectral libraries. However, because of the complexities of determining authentic (that is to say, pure or uncontaminated) spectra from specimens in which no pure spectra may be present in a given sample, various methods have been developed to extract such spectra from the dataset itself. Once the unmixing has taken place, the individual component images can be combined in a "composite" image, with control over the pseudo-color assigned to each plane.

Mansfield and colleagues (2005a,b) have outlined unique aspects of spectral unmixing methods that include "pure" spectral computation and automated spectral feature detection. "Compute Pure Spectrum" (CPS) is a mathematical tool that estimates the authentic spectrum of a fluorophore when its measured spectrum is contaminated by autofluorescence. The authors also describe automated pure spectral feature extraction ("Real Component Analysis" or RCA), a useful feature that not only assists in spectral library creation but can also serve as an exploratory aid that displays images corresponding to all detected spectral features, and in some cases can reveal unexpected components in unfamiliar specimens.

Quantitation. The unmixed images are typically presented to the user scaled for display—that is to say, stretched in such a way as to make dim signals visible. However, the underlying data are quantitative in the sense that the total signal measured at each pixel is assigned to each spectral channel as determined by each species' relative abundance. Thus, simple image analysis tools applied to each channel can be used to extract all relevant measures from regions of interest such as intensity (maximum, average, total), area, and dimension. In other words, while intensities measured at the camera may be related to "true"

signal intensity of an emitting object inside an animal in complicated ways, after the signals are captured at the sensor, subsequent multispectral analysis yields quantitatively accurate component-specific data.

Examples

In this section we illustrate the usefulness of multispectral imaging approaches for both macroscopic (in vivo) and microscopic samples.

Multispectral Small Animal Imaging

Multiplexing and Autofluorescence Removal (I)

A pair of nude mice imaged in the Maestro spectral imaging system (Figure 3) demonstrate the detection of faint fluorophore signals commingled with spectrally overlapping autofluorescence. The mice received subcutaneous injections of three fluorophores (FITC, TRITC, and Cy3.5), and they also exhibit both skin and food autofluorescence. The task is to detect and separate these overlapping fluorophores, which, except for FITC, are barely visible in the RGB image (top left). The inset, top center, shows the spectra of all five signals—skin autofluorescence (pink), and the extracted (estimated) spectra of FITC (green), TRITC (blue), Cy3.5 (red), and food (yellow)—generated using the "Compute Pure Spectrum" (CPS) tool. These spectra are consistent with their known spectral characteristics, as can be appreciated from the useful Omega Optical website (https://www.omegafilters.com/curvo2/index.php). The bottom panels, identified in the figure, illustrate the ability of spectral unmixing to separate the signals well isolated from each other; the images are shown as generated in the software, without further adjustments to brightness or contrast. The top right panel is a pseudo-colored composite image of the unmixed components.

Multiplexing and Autofluorescence Removal (II)

Figure 4 shows the striking results when different lymphatic drainage patterns are individually highlighted by appropriately located injections with different quantum dot (QD^1) species for each region. The top schematic indicates the location of each QD injection in an extremity of a nude mouse and shows the spectral characteristics of each quantum dot (as measured in the Maestro system). The center panels illustrate unmixing results after the quantum dots have spread through the lymphatics to arrive at the major draining nodes for each distribution. The left panel is simply the unmixed skin autofluorescence image, the center shows a composite image of the lymph nodes in situ after spectral unmixing, and the right is a composite image of these two components. The bottom panels show the results of imaging

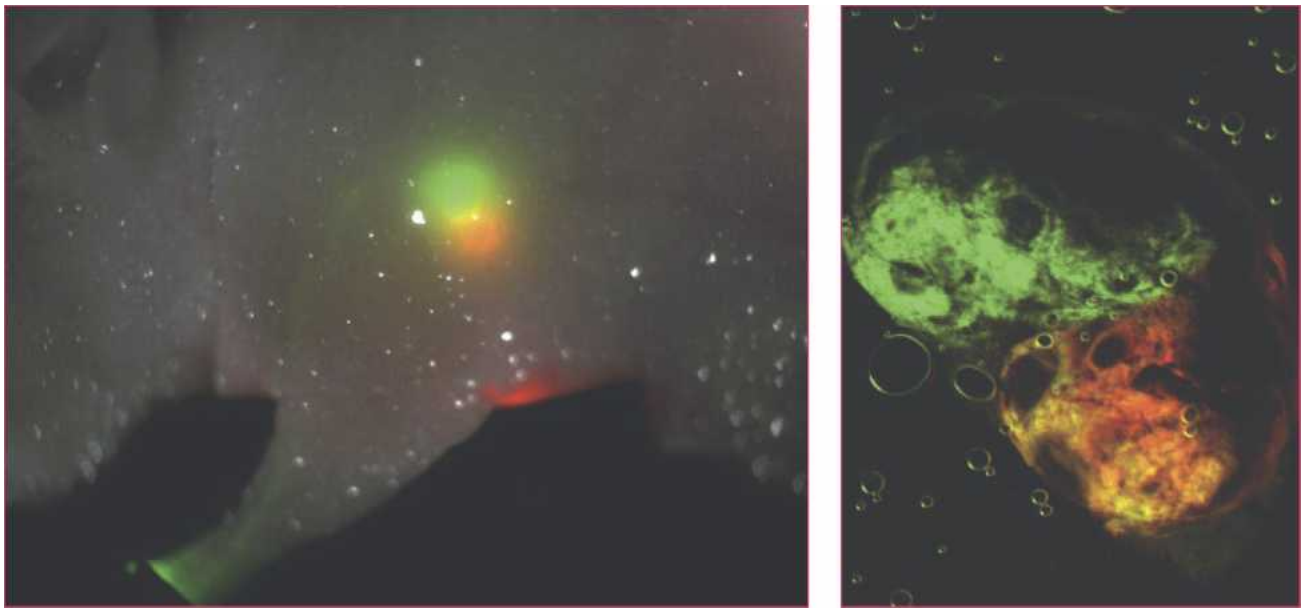

Figure 6 Combined macro- and micro-imaging of bidirectional axillary lymphatic flows from the mammary pad. A mouse was injected with 10 μL containing 12 pmol of 800-nm quantum dot (QD) (shown in green) intracutaneously into the middle digit of the left upper extremity and with 10 μL containing 12 pmol of 705-nm QD (shown in red) into the left mammary pad. Convergence of both drainage systems to the axillary region is shown in the left panel, a spectrally unmixed composite image. Fluorescence microscopy (right panel) demonstrates the distribution of the QD watershed of the two different lymphatic flows in individual lymph nodes.

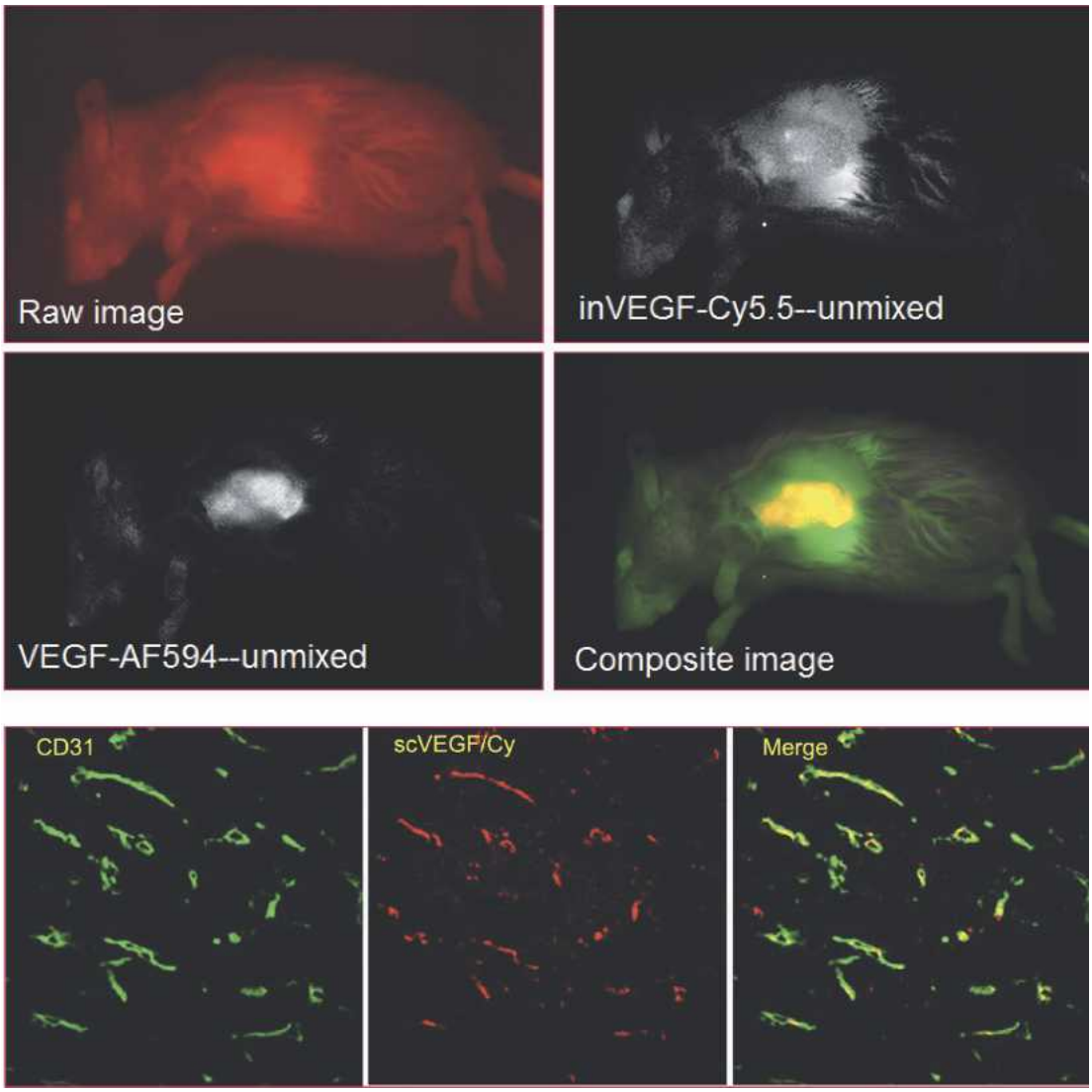

Figure 7 Combined macro- and micro-imaging of in vivo VEGF labeling of tumor. A Balb/c mouse bearing an orthotopic 4T1luc mouse mammary tumor was injected via the tail vein with an equimolar mixture of functionally active scVEGF/AlexaFluor-594 and inactivated inVEGF/Cy5.5 fluorescent conjugates. Spectral imaging reveals signals corresponding to inactive and active VEGF distribution as indicated. Microscopic analysis of a similar labeling experiment (but containing only active VEGF coupled to Cy5.5) is shown in the bottom panel. After in vivo labeling, the tumor was removed, cryosectioned, and immunostained for CD31 expression (a marker found on endothelial cell membranes). VEGF introduced in vivo is still visible in histological sections and co-localizes with CD31, as shown in the merged image on the right.

the nodes after surgical dissection (left, reflectance image; right, unmixed composite image).

Multispectral Microscopy

Multiplexing and Autofluorescence Removal in Microscopy

The sample shown in Figure 5 is a section of formalin-fixed, paraffin-embedded human prostate cancer specimen immunostained for prostate-specific antigen (PSA) and E-cadherin using indirect immunofluorescence with secondary antibodies (Invitrogen) conjugated to a 605-nm quantum dot (PSA) and a 655-nm quantum dot (E-cadherin). The slide was imaged at 10X from 500 to 800 nm with a Nuance imaging system. The top left panel is an RGB image reflecting the contribution of the QD signals plus autofluorescence. The bottom panels show the spectrum (as derived from this image) of the two QD species plus a tissue autofluorescence spectrum. Unmixing generated the three remaining bottom panels, indicating both the precise location of the two QD immunolabels and the ubiquitous presence of autofluorescence. Because these images are scaled for dis-

play, it is not possible to judge visually the relative intensities of the three channels, but quantitative analysis indicates that the autofluorescence signal is of the same order of magnitude as the PSA signals. Thus, without unmixing the contribution of the autofluorescence, accurate quantitation of each signal would have been compromised. The top right panel is a composite image of the two QD signals with the autofluorescence channel removed.

Implementing multispectral imaging on a microscope requires attention to two points. The first is that high-quality, apochromatic objectives do make a difference, especially in brightfield, since it is possible to see how badly typical mid-range achromats do when asked to be in focus from the blue all the way to the red and near-infrared. However, if the tuning range is restricted to green and above, most lenses are acceptable for spectral imaging applications. Second, for fluorescence, it is useful to replace the emission band-pass filters found in typical filter sets with long-pass filters.

Combining Small Animal Imaging and Microscopy (I)

The example shown in Figure 6 indicates the result of lymph drainage analysis using, in this case, two QD species, one injected in the left front paw and the other in the left mammary pad. The axillary lymph node received the two different lymphatic flows simultaneously. Spectral imaging was performed after the QD labels had an opportunity to reach their primary drainage nodes and, as can be seen in the left panel (in vivo image), the two QD signals both appeared in the axillary node region. Nodes from this region were subsequently dissected, and microscopic imaging confirmed that the two QD signals arose not just from the same region but from the same lymph node.

Combining Small Animal Imaging and Microscopy (II)

Figure 7 illustrates the use of active and related inactive molecular reagents in in vivo imaging. Such probe pairs can help distinguish molecularly targeted uptake and labeling from passive or unexpected binding. Balb/c mice bearing orthotopic 4T1luc mouse mammary tumors were injected via the tail vein with an equimolar mixture of functionally active single-chain (sc) VEGF/AlexaFluor-594 (scVEGF/Al) and inactivated inVEGF/Cy5.5 (inVEGF/Cy) fluorescent conjugates, a total of 20 μg per mouse. The scVEGF, labeled with fluorophores in such a way as not to inactivate the ligand, binds to VEGF receptors and is internalized via receptor-mediated endocytosis, while excessive random biotinylation of such conjugates completely abolishes binding and internalization (Backer et al. 2007).

Mouse images were obtained using a Maestro and processed with CRI software to obtain unmixed and composite images. Inactive VEGF distribution is shown in the top right panel; active VEGF distribution, localizing in the subcutaneous tumor, is shown in the center left panel; and the composite pseudo-colored image is presented in the center right. Microscopic analysis of a similar labeling experiment (but containing only active scVEGF coupled to Cy5.5) is shown in the bottom panel.

After in vivo labeling, the tumor was removed, cryosectioned, and immunostained for CD31 expression (a marker found on endothelial cell membranes). The bottom center panel shows that the labeled VEGF introduced in vivo is still visible in histological sections after sacrifice, and also in this case that its distribution mimics that of CD31, as revealed in the merged image on the right. This is a good illustration of how postmortem microscopy can and whenever possible should be used to validate in vivo labeling experiments.

We have shown here some examples of the benefits to multiplexed microscopy at the level of pixel co-registration. However, the data generated by this new imaging technology are not limited to pixel-level registration; with additional analysis and co-registration of other stains the data can be used to generate information at a cellular and subcellular level to provide true quantitative histocytometric information (Levenson 2006; Levenson and Mansfield 2006).

Conclusions

The field of small animal imaging is burgeoning, not only in its appeal to existing and new research constituencies but also in the wide and growing list of technologies at its disposal. To the established techniques that have migrated from the clinical to the preclinical arena (CT, MR, PET, SPECT, ultrasound) can be added techniques based on optical approaches. All of these technologies bring unique and in some cases complementary capabilities; here, we have focused on fluorescence-based optical techniques because of their combination of relatively low cost, high spatial resolution, good reagent flexibility, high throughput, and compatibility with relatively high levels of multiplexing. Many of these properties are enhanced by adding specific multispectral imaging capabilities.

We have given some examples of how multispectral approaches can improve overall sensitivity, especially when using fluorescent labels that emit in the visible range, where whole animal autofluorescence is strongest, and we have indicated the degree of in vivo multiplexing that is at least possible. The evolution of well-characterized and specific labeling reagents suitable for multiplexed experiments will help this field continue to develop.

Finally, we have sketched out how an integrated approach to whole animal imaging can involve postmortem validation of the imaging results by means of microscopic examination of relevant tissues. Multispectral approaches are of particular value here, especially when multiplexing is involved in vivo or is required in vitro to identify multiple tissue structures or cell types.

Acknowledgments

This work was partially supported by a Bioengineering Research Grant (1RO1 CA108468-01) and by the SBIR mechanism (1R44 CA88684), both through the National Institutes of Health.

References

Backer MV, Levashova Z, Patel V, Jehning BT, Claffey K, Blankenberg FG, Backer JM. 2007. Molecular imaging of VEGF receptors in angiogenic vasculature with single-chain VEGF-based probes. Nat Med 13:504-509.

Balaban RS, Hampshire VA. 2001. Challenges in small animal noninvasive imaging. ILAR J 42:248-262.

Berman JJ, Moore GW. 1994. Image analysis software for the detection of preneoplastic and early neoplastic lesions. Cancer Lett 77:103-109.

Del Guerra A, Damiani C, Di Domenico G, Motta A, Giganti M, Marchesini R, Piffanelli A, Sabba N, Sartori L, Zavattini G. 2000. An integrated PET-SPECT small animal imager: Preliminary results. IEEE T Nucl Sci 47:1537-1540.

Deroose CM, De A, Loening AM, Chow PL, Ray P, Chatziioannou AF, Gambhir SS. 2007. Multimodality imaging of tumor xenografts and metastases in mice with combined small-animal PET, small-animal CT, and bioluminescence imaging. J Nucl Med 48:295-303.

Farkas DL, Du C, Fisher GW, Lau C, Niu W, Wachman ES, Levenson RM. 1998. Non-invasive image acquisition and advanced processing in optical bioimaging. Comput Med Imaging Graph 22:89-102.

Gao X, Nie S. 2005. Quantum dot-encoded beads. Methods Mol Biol 303:61-71.

Gao X, Chan WC, Nie S. 2002. Quantum-dot nanocrystals for ultrasensitive biological labeling and multicolor optical encoding. J Biomed Opt 7:532-537.

Gao X, Cui Y, Levenson RM, Chung LW, Nie S. 2004. In vivo cancer targeting and imaging with semiconductor quantum dots. Nat Biotechnol 22:969-976.

Gat N. 2000. Imaging spectroscopy using tunable filters: A review. Proc SPIE 4056:50-64.

Graves EE, Ripoll J, Weissleder R, Ntziachristos V. 2003. A submillimeter resolution fluorescence molecular imaging system for small animal imaging. Med Phys 30:901-911.

Hoyt CC, Levenson RM, Banks PR. 2001. Novel high-sensitivity, high-throughput fluorescence polarization reader. Proc SPIE 4255:28-32.

Klibanov AL. 2005. Molecular imaging with targeted ultrasound contrast microbubbles. Ernst Schering Res Found Workshop: 171-191.

Lecchi M, Ottobrini L, Martelli C, Del Sole A, Lucignani G. 2007. Instrumentation and probes for molecular and cellular imaging. Q J Nucl Med Mol Imaging 51:111-126.

Levenson RM. 2006. Spectral imaging perspective on cytomics. Cytometry A 69:592-600.

Levenson RM, Mansfield JR. 2006. Multispectral imaging in biology and medicine: Slices of life. Cytometry A 69:748-758.

Mansfield JR, Gossage KW, Hoyt CC, Levenson RM. 2005a. Autofluorescence removal, multiplexing, and automated analysis methods for in-vivo fluorescence imaging. J Biomed Opt 10:41207.

Mansfield JR, Hoyt CC, Miller PJ, Levenson RM. 2005b. Distinguished photons: Increased contrast with multispectral in vivo fluorescence imaging. BioTechniques 39 (Suppl):S25-S29.

Miller PJ, Harvey AR. 2001. Signal to noise analysis of various imaging systems. Proc SPIE 4259:16-21.

Miller PJ, Hoyt CC. 1995. Multispectral imaging with a liquid crystal tunable filter. Proc SPIE 2345:354-365.

Miller JC, Fischman AJ, Aquino SL, Blake MA, Thrall JH, Lee SI. 2007. FDG-PET CT for tumor imaging. J Am Coll Radiol 4:256-259.

Nanni C, Di Leo K, Tonelli R, Pettinato C, Rubello D, Spinelli A, Trespidi S, Ambrosini V, Castellucci P, Farsad M, Franchi R, Pession A, Fanti S. 2007. FDG small animal PET permits early detection of malignant cells in a xenograft murine model. Eur J Nucl Med Mol Imaging 34:755-762.

Ntziachristos V, Hielscher AH, Yodh AG, Chance B. 2001. Diffuse optical tomography of highly heterogeneous media. IEEE Trans Med Imaging 20:470-478.

Ntziachristos V, Bremer C, Graves EE, Ripoll J, Weissleder R. 2002. In vivo tomographic imaging of near-infrared fluorescent probes. Mol Imaging 1:82-88.

Ntziachristos V, Bremer C, Weissleder R. 2003. Fluorescence imaging with near-infrared light: New technological advances that enable in vivo molecular imaging. Eur Radiol 13:195.

Ntziachristos V, Ripoll J, Wang LV, Weissleder R. 2005. Looking and listening to light: The evolution of whole-body photonic imaging. Nat Biotechnol 23:313-320.

Postema M, Bouakaz A, Versluis M, de Jong N. 2005. Ultrasound-induced gas release from contrast agent microbubbles. IEEE T Ultrason Ferr 52:1035-1041.

Rice BW, Cable MD, Nelson MB. 2001. In vivo imaging of light-emitting probes. J Biomed Opt 6:432-440.

Taylor CR, Levenson RM. 2006. Quantification of immunohistochemistry—issues concerning methods, utility and semiquantitative assessment II. Histopathology 49:411-424.

Torigian DA, Huang SS, Houseni M, Alavi A. 2007. Functional imaging of cancer with emphasis on molecular techniques. CA Cancer J Clin 57: 206-224.

Troy T, Jekic-McMullen D, Sambucetti L, Rice B. 2004. Quantitative comparison of the sensitivity of detection of fluorescent and bioluminescent reporters in animal models. Mol Imaging 3:9-23.

van der Weerdt AP, Boellaard R, Visser FC, Lammertsma AA. 2007. Accuracy of 3D acquisition mode for myocardial FDG PET studies using a BGO-based scanner. Eur J Nucl Med Mol Imaging 34:1439-1446.

Weissleder R, Mahmood U. 2001. Molecular imaging. Radiology 219:316-333.

Wolz G, Nomayr A, Hothorn T, Hornegger J, Romer W, Bautz W, Kuwert T. 2007. Anatomical accuracy of interactive and automated rigid registration between X-ray CT and FDG-PET. Nuklearmedizin 46:43-48.

Zhang HF, Maslov K, Stoica G, Wang LV. 2006. Functional photoacoustic microscopy for high-resolution and noninvasive in vivo imaging. Nat Biotechnol 24:848-851.

Zhang HF, Maslov K, Wang LV. 2007. In vivo imaging of subcutaneous structures using functional photoacoustic microscopy. Nat Protoc 2: 797-804.